2009 International Conference on Embedded Software and Systems

RBFNN Aided Extended Kalman Filter for MEMS AHRS/GPS

Linlin Xia, Jianguo Wang
School of Automation Engineering
Northeast Dianli University
Jilin, China
xiall521@mail.nedu.edu.cn

Gangui Yan *IEEE Member*
Electrical Engineering College
Northeast Dianli University
Jilin, China
yangg@mail.nedu.edu.cn

***Abstract*—A Radial Basis Function Neural Network (RBFNN)-aided Extended Kalman Filter (EKF) is designed towards a low cost solid-state integrated navigation system. This system incorporates measurements from an attitude and heading reference system (AHRS) and a GPS, providing unaided, complete and accurate navigation information for land vehicles. To realize the EKF algorithm, the architectures of this AHRS/GPS and the description of Pseudo_range- Pseudo_range Rate -Heading measurements model are intensively illustrated. In sequence, the fundamentals of radial basis function (RBF) technique are discussed by the procedure of aiding mode and realization process. The simulation test shows when the carrier is in dynamic environment, the navigation parameters are relatively precise, even if the accuracy of the sensors is modest. This fusion filter approach, illustrated here proves to be a practical approach for navigation parameters estimation in real time.**

Keywords-EKF; RBFNN; fusion filter; AHRS/GPS; Pseudo_range- Pseudo_range Rate -Heading measurements

I. INTRODUCTION

AHRS is generally used for aviation applications, providing the on-the-movement attitude and heading estimation for carriers. In this work, a low cost solid-state AHRS/GPS is framed by incorporating a GPS receiver, an AHRS and a navigation computer, offering complete navigation information including stabilized position, velocity and attitude to georeference a land vehicle at any moment of time. Here, the AHRS is structured based on the Micro Electro Mechanical System (MEMS) technology, which presents the prominent characteristics of small volume, light weight, high reliability and strong shock-resistantance.

Global Position System (GPS) has been widely used in the field of space explore, land geodesy, and ocean geophysics during these decades, which has become the primary positioning solution for the land vehicular navigation. Due to the outstanding all-weather available orientation technology, GPS mostly contributes to compose the combination systems together with other assisted navigation sub-systems, inertial navigation system (INS)/GPS integration manner is regarded as a classical one.

The extended Kalman filter (EKF) is the key means when solving data fusion issues of integrated navigation system. In the field of tightly-coupled AHRS/GPS, the state model of this system is a linear one, on contrast, the measurement model contains components that are nonlinear in nature, so a real-time EKF filter is necessary to be constructed, approaching the nonlinear components according to Taylor Expansion Theory.

Due to the large drifts and poor stability of MEMS inertial sensors, the fusion filter solution with high rapid, effective, high robustness, and high accuracy is proposed, which fuses the EKF methods and artificial intelligent (AI) ones based on artificial networks, achieving the optimal estimates of full navigation parameters for moving bodies.

The net suits for this occasion should possess the following features:

1) According to the estimates correction for every filter period, the number of training sampling is huge enough, so the number of the basis functions should much smaller than that of the sampling.

2) The selected net for this work should be able to approach the nonlinear function.

3) The nodes for the input and output layers should be equal, namely, the dimensions of the state are equal.

4) As the net have not to provide the feedback information for the estimated state, the forward (no-feedback) net structure should be fine.

Considering the limited conditions mentioned above, the generalized radial basis function neural network (RBFNN) is selected to modify the predicted states on line. The aiding procedure contains two steps, namely, training offline and correction online.

The outline of the remainder of the paper is as follows. In the following section, the AHRS stand-alone working mode is established. The combination mode of AHRS/GPS is described in section III, we emphasize on the system state model and measurement model. In section IV, the RBFNN navigation correction is introduced to this issue. Section V carries on the numerical simulation to assess the performance of RBFNN aided EKF algorithm applied to this AHRS/GPS. Section VI contains the main results of the investigation.

II. STAND-ALONE AHRS STRATEGY MODE

As a mature commercial product, the AHRS can fulfill the navigation task in the stand-alone mode. The whole system is normally established with micro electronic

978-0-7695-3678-1/09 $25.00 © 2009 IEEE
DOI 10.1109/ICESS.2009.42

mechanical system (MEMS) measurement units, namely three MEMS gyros, three MEMS accelerometers and three miniature magnetic sensors, accomplishing comprehensive information of angular rate, acceleration and magnetic field intensity of body tri-axes respectively, which then define the attitude and heading angles estimates in real time. The block diagram of this system is given in Fig.1.

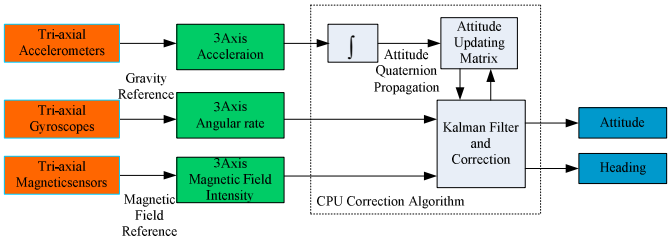

Figure 1. Block diagram of AHRS

In this AHRS, the accurate attitude sensing is accomplished by measuring acceleration in three orthogonal axes to complete roll and pitch attitude reference relative to the gravity vector; heading is obtained by computing the heading angle reference about the Z-axis relative to the earth's magnetic field vector, which helps to compensate the drifts of the mid-level grade of MEMS rate gyros in real time.

III. AHRS/GPS Mode Description

When a miniature GPS receiver is added to an AHRS, the combined system becomes a low-cost solid state INS/GPS integration, which can provide the full navigation information involving attitude, velocity and location to moving bodies. Differing from the conventional INS, the estimate of heading angle is obtained from magnetic sensors' outputs, GPS realizes the measurements of position and velocity, the accelerometers, however, are not used as a direct attitude reference, and only used in the propagation of the velocity vector [1]. The block diagram of the tightly-couple AHRS/GPS architecture is shown in Fig. 2.

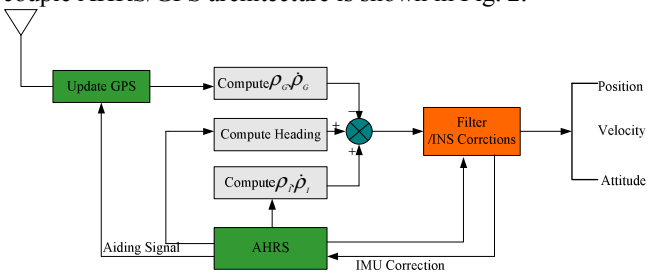

Figure 2. Block diagram of AHRS/GPS architecture

A. System State Model

Denote the navigation coordinate frame by $E-N-U$, E , N , U express the east, north and up respectively. Let $X(t)$ is the system state model, as the estimates of vertical velocity and altitude are not necessary for land vehicles, then

$$X(t)=\left[\delta L\ \delta\lambda\ \delta V_E\ \delta V_N\ \phi_E\ \phi_N\ \phi_U\ \varepsilon_x\ \varepsilon_y\ \varepsilon_z\ \nabla_x\ \nabla_y\ \nabla_z\ \delta t_r\ \delta t_f\right]^T$$

Where $X(t)\in R^{15}$, $\delta L,\delta\lambda$ express the latitude and longitude error respectively; $\delta V_E,\delta V_N$ express the east and north velocity error respectively; ϕ_E,ϕ_N,ϕ_U express the attitude angle error of navigation plat respectively; ε^b and ∇^b express the drift vector of MEMS gyros and the bias vector of MEMS accelerometers in the body frame; δt_r is the receiver clock bias in meters, δt_f is the receiver clock frequency bias in meters per second, and define

$$\varepsilon^b=\left[\varepsilon_x\ \ \varepsilon_y\ \ \varepsilon_z\right]^T \tag{1}$$

$$\nabla^b=\left[\nabla_x\ \ \nabla_y\ \ \nabla_z\right]^T \tag{2}$$

$$\dot{\varepsilon}^b=F_{gyro}\varepsilon+W_\varepsilon \tag{3}$$

$$\dot{\nabla}^b=F_{acc}\nabla+W_\nabla \tag{4}$$

$$F_{gyro}=-diag\left[1/\tau_{\varepsilon x}\ \ 1/\tau_{\varepsilon y}\ \ 1/\tau_{\varepsilon z}\right] \tag{5}$$

$$F_{acc}=-diag\left[1/\tau_{\nabla x}\ \ 1/\tau_{\nabla y}\ \ 1/\tau_{\nabla z}\right] \tag{6}$$

$$\dot{\delta t}_r=\delta t_f \tag{7}$$

$$\dot{\delta t}_f=-\alpha\delta t_f+W_{t_f} \tag{8}$$

Where, τ_ε and τ_∇ denote time constants relating to the gyros' drifts and accelerometers' bias respectively; F_{gyro} and F_{acc} are both defined as the diagonal matrixes. α is the anti-correlated time parameter relating to the receiver clock bias; δt_r is the receiver clock bias in meters; δt_f is the receiver clock frequency bias in meters per second; W_ε , W_∇ ,and W_{t_f} are all white noise.

B. System Measurement Model

Denote the position and velocity vector extracted from the AHRS by $(x_I,y_I,z_I)^T$, and $r_I=(\dot{x}_I,\dot{y}_I,\dot{z}_I)^T$ respectively. Let the true position vector of the moving vehicle is $(x,y,z)^T$, and let the satellite position vector obtained from the j th satellite message is $\left(x_s^j,y_s^j,z_s^j\right)^T$.

Denote the Pseudo_range obtained from the AHRS and satellites position by ρ_I ($\dot{\rho}_I$ for Pseudo_range Rate). Let the pseudo_range obtained from the GPS receiver is ρ_G^j , and $\dot{\rho}_G^j$ for GPS Pseudo_range Rate.

1) Pseudo_range Measurement Equation

The pseudo_range measurements of GPS receiver can be written as:

$$\rho_G^j=\rho^j+\delta t_r+v_\rho^j\quad(j=1,2,\cdots,n) \tag{9}$$

Where $\rho^j=\sqrt{(x-x_{sj})^2+(y-y_{sj})^2+(z-z_{sj})^2}$ being the actual range between the satellites and the moving vehicle. n is the available number of the satellites. v_ρ^j is the

composite of measurement errors associated with the j th satellite, which can been seen as white noise.

In a similar fashion, the pseudo_range obtained from the AHRS and the j th available satellites position can be written as the following expression:

$$\rho_I^j = \sqrt{(x_I - x_s^j)^2 + (y_I - y_s^j)^2 + (z_I - z_s^j)^2} \qquad (10)$$

Let the position error vector is $(\delta x, \delta y, \delta z)^T$, then we get

$$x_I = x + \delta x \,,\; y_I = y + \delta y \,,\; z_I = z + \delta z$$

Expanding (10) according to Taylor equations at point (x, y, z), and omitting the complicated high-order terms, we can rewrite (10) by the following expression:

$$\rho_I^j = \rho^j + \frac{\partial \rho^j}{\partial x}\delta x + \frac{\partial \rho^j}{\partial y}\delta y + \frac{\partial \rho^j}{\partial z}\delta z \qquad (11)$$

And assume that $(x - x_{sj})/\rho^j = e_{jx} = \cos\alpha_{sj}$, $(y - y_{sj})/\rho^j = e_{jy} = \cos\beta_{sj}$, $(z - z_{sj})/\rho^j = e_{jz} = \cos\gamma_{sj}$. Where, α_{sj} , β_{sj} , γ_{sj} stand for the included angles between the direction vector relating vehicle body to the j th satellite and tri-axes of the earth frame.

(21)- (1), the difference between these two Pseudo_ranges can be described as

$$\delta\rho^j = \rho_I^j - \rho_G^j = e_{jx}\delta x + e_{jy}\delta y + e_{jz}\delta z \qquad (12)$$

For the land vehicular bodies, we have not to take the vertical height and vertical velocity into consideration, which means that 3 available satellites are sufficient, namely $j = 1,2,3$.

Establishing the relationship of position error vector in ECEF coordinate frame and geodetic (g-) coordinate frame:

$$\delta r = \begin{bmatrix} \delta x \\ \delta y \\ \delta z \end{bmatrix} = D_A \cdot \begin{bmatrix} \delta L \\ \delta \lambda \end{bmatrix} \qquad (13)$$

According to the observation equation of the standard EKF:

$$Z_1(t) = H_1(t)X(t) + V_1(t) \qquad (14)$$

Where, $Z_1(t) = \begin{bmatrix} \delta\rho^1 & \delta\rho^2 & \delta\rho^3 \end{bmatrix}^T$, $H_1(t) = \begin{bmatrix} e \cdot D_A & 0_{3\times 11} & K & 0_{3\times 1} \end{bmatrix}$, $V_1(t) = V_\rho = \begin{bmatrix} -v_{\rho^1} & -v_{\rho^2} & -v_{\rho^3} \end{bmatrix}^T$, $e = \begin{bmatrix} e_{1x} & e_{1y} & e_{1z} \\ e_{2x} & e_{2y} & e_{2z} \\ e_{3x} & e_{3y} & e_{3z} \end{bmatrix}$ being a known matrix, $D_A = \begin{bmatrix} -R_N \sin L\cos\lambda & -R_N \cos L\sin\lambda \\ -R_N \sin L\sin\lambda & R_N \cos L\cos\lambda \\ R_N(1 - f^2)\cos L & 0 \end{bmatrix}$, $K_{3\times 1} = \begin{bmatrix} -1 & -1 & -1 \end{bmatrix}^T$.

2) Pseudo_range Rate Measurement Equation

Let the true velocity vector of the vehicle body is $(\dot{x}, \dot{y}, \dot{z})^T$, the satellite velocity vector obtained from the j th satellite message is $(\dot{x}_s^j, \dot{y}_s^j, \dot{z}_s^j)^T$. Let the GPS pseudo_range rate is $\dot{\rho}_G^j$, which is measured by the Doppler in practice [2], define the pseudo_range rate is as follows:

$$\dot{\rho}_G^j = \dot{\rho}^j + \delta t_f + v_{\dot{\rho}^j} \quad (j = 1, \cdots, n) \qquad (15)$$

Where

$$\dot{\rho}^j = \left[(x - x_{sj})(\dot{x} - \dot{x}_{sj}) + (y - y_{sj})(\dot{y} - \dot{y}_{sj}) + (z - z_{sj})(\dot{z} - \dot{z}_{sj})\right] / \rho^j$$

being the true range rate value. $v_{\dot{\rho}^j}$ is pseudo_range rate measurements noise modeled as white noise.

Denote the pseudo_range range obtained from the AHRS and the j th available satellites position by $\dot{\rho}_I^j$, the corresponding expression is

$$\dot{\rho}_I^j = \left[(x_I - x_{sj})(\dot{x}_I - \dot{x}_{sj}) + (y_I - y_{sj})(\dot{y}_I - \dot{y}_{sj}) + (z_I - z_{sj})(\dot{z}_I - \dot{z}_{sj})\right] / \rho_I^j \qquad (16)$$

Let the velocity error that AHRS gives in the ECEF coordinate frame is $(\delta\dot{x}, \delta\dot{y}, \delta\dot{z})^T$, then

$$\dot{x}_I = \dot{x} + \delta\dot{x} \,,\quad \dot{y}_I = \dot{y} + \delta\dot{y} \,,\quad \dot{z}_I = \dot{z} + \delta\dot{z}$$

In a similar fashion, Expanding (15) to be a Taylor series form at point $(x, y, z, \dot{x}, \dot{y}, \dot{z})$, and omitting high-order terms, the result is given approximately by

$$\dot{\rho}_I^j = \dot{\rho}^j + \frac{\partial \dot{\rho}^j}{\partial x}\delta x + \frac{\partial \dot{\rho}^j}{\partial y}\delta y + \frac{\partial \dot{\rho}^j}{\partial z}\delta z + \frac{\partial \dot{\rho}^j}{\partial \dot{x}}\delta\dot{x} + \frac{\partial \dot{\rho}^j}{\partial \dot{y}}\delta\dot{y} + \frac{\partial \dot{\rho}^j}{\partial \dot{z}}\delta\dot{z} \qquad (17)$$

Where, $g_{jx} = \frac{\dot{x} - \dot{x}_{sj}}{\rho^j} - \frac{\dot{\rho}^j}{(\rho^j)^2}(x - x_{sj})$, $g_{jy} = \frac{\dot{y} - \dot{y}_{sj}}{\rho^j} - \frac{\dot{\rho}^j}{(\rho^j)^2}(y - y_{sj})$, $g_{jz} = \frac{\dot{z} - \dot{z}_{sj}}{\rho^j} - \frac{\dot{\rho}^j}{(\rho^j)^2}(z - z_{sj})$.

(17)- (15), the difference between these two Pseudo_range rate is

$$\delta\dot{\rho}^j = \dot{\rho}_I^j - \dot{\rho}_G^j = e_{jx}\delta\dot{x} + e_{jy}\delta\dot{y} + e_{jz}\delta\dot{z} + g_{jx}\delta x + g_{jy}\delta y + g_{jz}\delta z \qquad (18)$$

Establishing the relationship of V^n (velocity in g-coordinate frame) and V^e (velocity in ECEF coordinate frame), namely [3]

$$V^e = C_n^e V^n \qquad (19)$$

Where, $C_n^e(L, \lambda) = \begin{bmatrix} -\sin\lambda & -\sin L\cos\lambda \\ \cos\lambda & -\sin L\sin\lambda \\ 0 & \cos L \end{bmatrix}$. We get the differential equation

$$\delta V^e = \delta(C_n^e)V^n + C_n^e \delta V^n \qquad (20)$$

And

$$\delta(C_n^e)V^n = D_e \cdot \begin{bmatrix} \delta L \\ \delta\lambda \end{bmatrix} \qquad (21)$$

Substituting (21) into (20), we obtain

$$\begin{bmatrix}\delta\dot{x}\\ \delta\dot{y}\\ \delta\dot{z}\end{bmatrix}=D_e\begin{bmatrix}\delta L\\ \delta\lambda\end{bmatrix}+C_n^e\begin{bmatrix}\delta V_E\\ \delta V_N\end{bmatrix} \tag{22}$$

Where,

$$D_e=\begin{bmatrix}-V_N\cos L\cos\lambda & -V_E\cos\lambda+V_N\sin L\sin\lambda\\ -V_N\cos L\sin\lambda & -V_E\sin\lambda-V_N\sin L\cos\lambda\\ -V_N\sin L & 0\end{bmatrix}.$$

We can get the aim function, namely

$$Z_2(t)=H_2(t)X(t)+V_2(t) \tag{23}$$

Where, $Z_2(t)=\begin{bmatrix}\delta\dot{\rho}^1 & \delta\dot{\rho}^2 & \delta\dot{\rho}^3\end{bmatrix}^T$,

$H_2(t)=\begin{bmatrix}(g\cdot D_A+e\cdot D_e) & e\cdot C_n^e & 0_{3\times10} & K\end{bmatrix}$,

$g=\begin{bmatrix}g_{1x} & g_{1y} & g_{1z}\\ g_{2x} & g_{2y} & g_{2z}\\ g_{3x} & g_{3y} & g_{3z}\end{bmatrix}$ being a known matrix,

$V_2(t)=V_{\dot{\rho}}=\begin{bmatrix}-v_{\dot{\rho}^1} & -v_{\dot{\rho}^2} & -v_{\dot{\rho}^3}\end{bmatrix}^T$.

3) Heading Measurement Equation

As the whole system shows great dependence on the magnetic field vector, the residual between the magnetic sensors' reading and the calculated reading from AHRS can be constructed as [4]

$$\delta\psi=\psi_1\pm D-\hat{\psi}=-\phi_U \tag{24}$$

Where, ψ_1 stands for the magnetic heading in geodetic coordinate frame, D is the local magnetic declination between geodetic north and magnetic north, and $\hat{\psi}$ is the calculated heading from AHRS, then

$$z_3(t)=\delta\psi=-\phi_U \tag{25}$$

The measurement equation of this sub-system can be described as

$$Z_3(t)=H_3(t)X(t)+V_3(t) \tag{26}$$

Where, $H_3(t)=\begin{bmatrix}0_{1\times6} & -1 & 0_{1\times8}\end{bmatrix}$.

Composing (14), (23), (26), the final measurement equation can be given by

$$Z(t)=\begin{bmatrix}Z_1(t)\\ Z_2(t)\\ Z_3(t)\end{bmatrix}_{7\times1} \tag{27}$$

IV. RBF Neural Network Aided Filter Design

In this section, the radial basis function neural network (RBFNN) aided navigation solution is introduced to fulfill an on-the-movement calibration of AHRS/GPS. Let's go to the related theory of RBFNN. Choosing the Gauss function as the activation radial basis function for the hidden layer, namely

$$g_i(x)=g_i(\|x-c_i\|)=\exp\left(-\frac{\|x-c_i\|^2}{2\sigma_i^2}\right)\quad i=1,2,\cdots,I \tag{28}$$

Where, $g_i(x)$ is the Gauss function, $c_i\in R^I$ being centers of the basis functions, I is the number of the radial basis function, $\|\cdot\|$ denotes norm that is usually taken to be Euclidean distance, σ_i is the width vector of the Gauss function [5]. The output function of this net can be described as (for the k-th neuron):

$$F_k(x)=\sum_{i=1}^{I}w_{ik}g_i(x)\qquad k=1,2,\cdots,m \tag{29}$$

Where, m is the neuron number of the input layer, ω_{ik} is the weight vector between hidden layer and output layer. The topology architecture of the RBFNN is given in Fig.3.

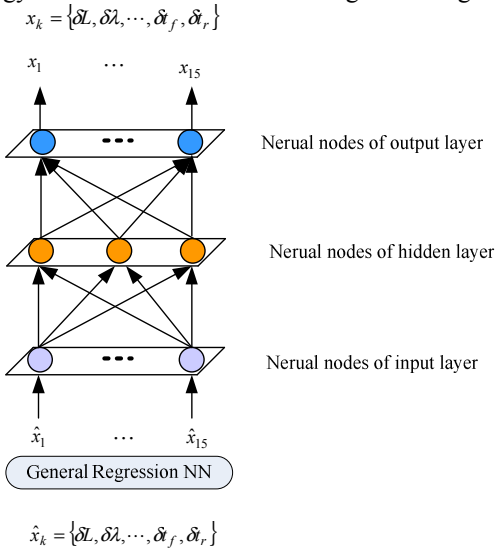

Figure 3. Topology of RBF neural network

Where, $\hat{x}_k=(\delta L,\delta\lambda,\cdots,\delta v_f,\delta v_r)^T\in R^{15}$ being the input vector, which stands for the predict value of the state, $x_k=(\delta L,\delta\lambda,\cdots,\delta v_f,\delta v_r)^T\in R^{15}$ being the output vector, which stands for the expected estimate state of this AHRS/GPS navigation system, namely, $m=15$. Choosing general regression neural network (GRNN) with 3 neurons in hidden layer as training net, namely, $I=3$, then the net structure is 15-3-15. Through a lot of simulation, we finally adopt three Gauss functions, $g_i(c_i,\sigma_i)$: $g_1(x)=(0,0.1)$, $g_2(x)=(1.5,0.1)$, $g_3(x)=(-2,0.1)$, and the initial weight are set as $w_{1k}=1$, $w_{2k}=1$, $w_{3k}=0.5$ respectively. The whole training procedure includes two sub- processes.

A. Training Offline

Choosing $\hat{x}_k$, x_k as the training input and output respectively, the training stylebook are coming from the real-time estimate state of EKF, which could be very large (1800 samples), and this is one of the reasons that why we choose the RBFNN. After a series of offline training process, we get the net outputs $\bar{x}_k$, and define

$$\Delta E=\bar{x}_k-\hat{x}_k \tag{30}$$

Where, $\Delta E\in R^{15}$ is the error between real-time estimated state $\hat{x}_k$ coming from the state equation and the real-time net estimated state $\bar{x}_k$ coming from the

complicated mapping process. Saving this error information into the parameter model database, and when the simulation goes to the online-correction, we just remove the corresponding error on the sampled-time. That is, we can realize the online-correction of the state equations by this artificial networks technology.

B. *Correction Online*

After all the offline training process, we define a parameter $\bar{x}_k$, which stands for the predict state of the modified state equation, then

$$\bar{x}_k = \hat{x}_k + \Delta E = \bar{x}_k \tag{31}$$

In this step, we can modify the value of the estimated state by the trained net on real time. Substituting $\bar{x}_k$ for the state parameter $\hat{x}_k$ in the following EKF process, and rewriting the covariance matrix, gain matrix and update estimate of state, we can rebuild the filter computation. The block diagram of the RBFNN aided STQEKF is given by Fig.4.

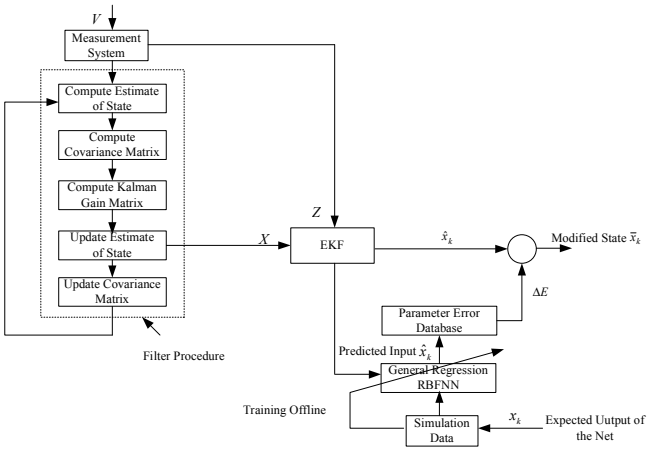

Figure 4. Block diagram of the fusion filter

The fusion filter includes two steps:

1) Realizing the standard EKF calculation, we get the estimated state $\hat{x}_k$.

2) Obtaining the modified state $\bar{x}_k$ aided by RBFNN online correction, substituting $\bar{x}_k$ for $\hat{x}_k$ in the following training process.

V. NUMERICAL SIMULATION

A. *Simulation Environment*

Numerical simulation is carried out to confirm the performance of the RBFNN Aided EKF algorithm. The collected GPS data is obtained from National Geodetic Survey [6], and let SV02, SV06 and SV11 (poor GDOP solution) are visible satellites. Suppose that the average acceleration of the moving body is $a = 0.1g$, the body plat base is in the mode of lateral and vertical swing, the initial velocity is $V_{E0} = V_{N0} = 10$m/s, and the initial position is $L_0 = 45.78°$, $\lambda_0 = 126.67°$. The threshold navigation condition is designed as follows: The initial longitude and latitude error are all 0.001°, the initial velocity errors are all 0.05m/s, and the initial attitude errors are 0.5°, 0.5°, and 3° respectively. As for GPS, the receiver clock bias is 30m (1σ), the receiver clock bias is 0.05m/s (1σ), and time parameter relating to receiver clock bias is $\alpha = 0.001$. The initial attitude quaternion is $q=(1,0,0,0)^T$, and its propagation is implemented with 4 order Runge-kutta algorithm. The local acceleration vector is set as $a_0 = [0 \;\; 0 \;\; -9.78049]^T$ m/s^2, and the magnetic field vector is set as $m_0 = 1.5\times10^{-6}\cdot[1 \;\; 0 \;\; 1]^T$ T (which can be obtained from IGRF [7] with the real-time longitude, latitude and altitude). As the GPS outage is tied to 1pps (one pulse per second), the AHRS sample period is 0.01s, so the filter period is sampled as T_f=1.0s. The total time for simulation is 1800s. The corresponding initial estimates of the micro measurement units involved are listed in table I.

TABLE I
INITIAL ESTIMATES FOR MICOR SENSORS

Measurement unit	Constant drifts	Random noise	Related time constant
Gyro	100 deg/h	10 deg/h	3600s
Accelerometer	1000 μg	500 μg	1800s
Fluxgate sensor	1500 nT	150 nT	

B. *Results and Analysis*

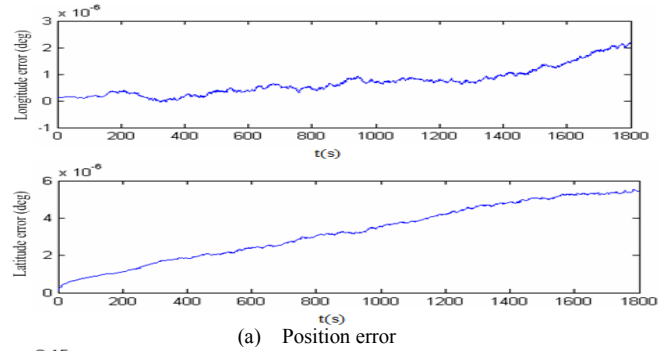

(a) Position error

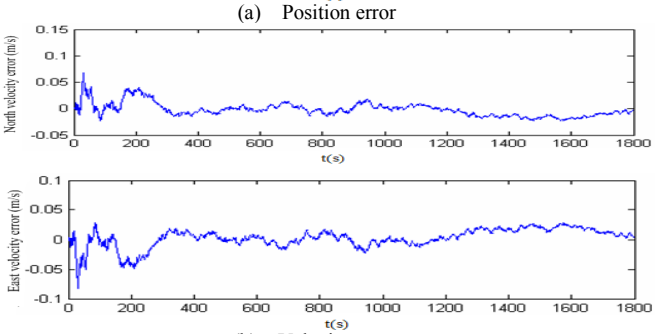

(b) Velocity error

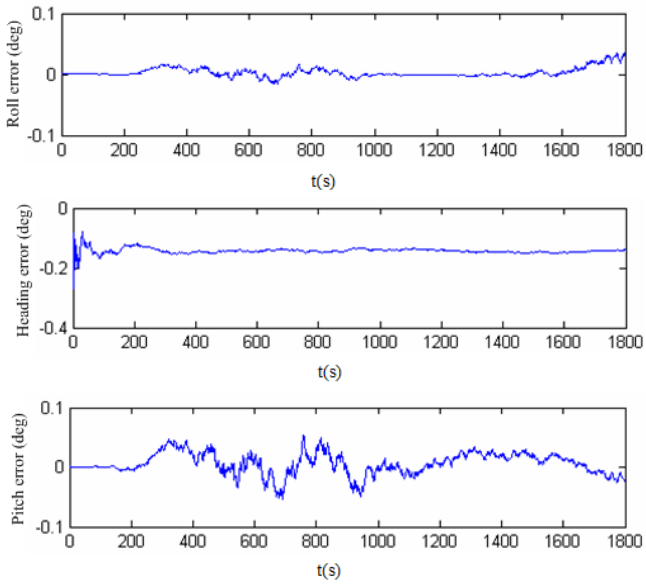

(c) Attitude error

Figure5. parameter estimates by using RBFNN aided EKF approach

TABLE II
ROOT MEAN SQUARE OF ESTIMATES ERROR FOR TWO DESIGN OPTIONS

RMS	Attitude error (")			Position error (m)		
	Pitch	*Roll*	*Head-ing*	*X-axial*	*Y-axial*	*Z-axial*
EKF	114.12	33.48	36.36	3.68	1.52	3.31
RBF Aided EKF	100.08	32.04	34.92	3.38	0.92	2.11
Control Effect	12.3%	4.3%	4.0%	8.2%	39.5%	33.2%

Both sets of data, which includes the GPS measurements (position and velocity in ECEF) and the sensor measurements (gyros and accelerometers in the body frame), were then used as inputs into a GPS/AHRS numerical simulation. Figure.5 shows the simulation results of the navigation parameter, (a), (b) and (c) are the position, velocity and attitude error filter curve respectively. As we can see from the figures, the attitude error is within -0.4~ 0°, the velocity error is below 0.2 m/s, and the position error never exceeds 10^{-5} °.

The comparison of performances of RBFNN aided EKF and standard EKF are demonstrated through the root mean square (RMS) data of the navigation parameters, as they are shown in table II. The attitude error is described in second, given in navigation coordinate frame, and the position error is given in ECEF coordinate frame. It is cleared that the fusion filter leads to more accurate estimates than the standard EKF at a significant cost decrease of the tactical inertial sensors(for gyros,10deg/h), and the control effect increased 4.0% to 39.5%.

VI. CONCLUSION

An ANN aided extended Kalman filter is constructed towards a solid-state AHRS/GPS, which fuses measurements data including acceleration, angular rate, magnetic field intensity, and the position/velocity in ECEF frame. Considering the large training sample and no-feedback net structure, the generalized radial basis function neural network (RBFNN) is selected to modify the predicted states on line. The principle of the training offline and the correction online is described by mathematics model. The numerical simulation is established to validate the performance of the fusion filter solution; in consequence, the accuracy and kinematic performance are all enhanced as expected, compared to the pure EKF model. Study has shown that the fusion filtering is feasible for parameter estimates in the field of low cost AHRS/GPS, even if the accuracy of the sensors is modest.

ACKNOWLEDGMENT

The financial support from The Doctor Scientific Research Fund of Northeast Dianli University under the grant No. BSJXM-200801 is gratefully acknowledged.

REFERENCES

[1] Jose A. Rios, Elecia White, "Fusion filter algorithm enhancements for a MEMS GPS/IMU," *ION NTM,* San Diego, California, USA, Jan 2002.

[2] Zhao Lin, "Satellite Navigation Systems." *Harbin Engineering University Publishing Company*, 2001.

[3] Jing Yang, Hongyue Zhang, Shiqing Zhu. "GPS/SINS fault tolerant integrated navigation system based on pseudo-range and its rate", *Airspace Control*, vol. 21, pp. 17-23, 2003.

[4] Zhao Lin, Xia Lin-lin, Liu Fan-ming, Cheng Yi, "Application of UKF for MEMS IMUs and fluxgate sensors based attitude and heading reference systems of carriers." *2nd IEEE Conference on Industrial Electronics and Applications,* pp. 2278-2283, May 2007.

[5] Simon Haykin, "Neural Networks." *China Machine Press*, 2005.

[6] National Geodetic Survey. Sep 1, 2007. http://www.ngs.noaa.gov.

[7] National Geophysical Data Center. April 25, 2007. http:// www.ngdc.noaa.gov/IAGA/vmod/igrf.html.